APL Materials

Deep acceptors and their diffusion in Ga_2O_3

Cite as: APL Mater. **7**, 022519 (2019); https://doi.org/10.1063/1.5063807
Submitted: 01 October 2018 . Accepted: 04 December 2018 . Published Online: 08 January 2019

Hartwin Peelaers, John L. Lyons, Joel B. Varley, and Chris G. Van de Walle

Deep acceptors and their diffusion in Ga_2O_3

Cite as: APL Mater. 7, 022519 (2019); doi: 10.1063/1.5063807
Submitted: 1 October 2018 • Accepted: 4 December 2018 •
Published Online: 8 January 2019

Hartwin Peelaers,[1,2,a)] John L. Lyons,[3] Joel B. Varley,[4] and Chris G. Van de Walle[1]

AFFILIATIONS

[1] Materials Department, University of California, Santa Barbara, California 93106-5050, USA
[2] Department of Physics and Astronomy, University of Kansas, Lawrence, Kansas 66045, USA
[3] Center for Computational Materials Science, US Naval Research Laboratory, Washington, DC 20375, USA
[4] Lawrence Livermore National Laboratory, Livermore, California 94550, USA

[a)] **Electronic mail:** peelaers@ku.edu

ABSTRACT

β–Ga_2O_3 is a wide-bandgap material with promising applications in high-power electronics. While n-type doping is straightforward, p-type doping is elusive, with only deep acceptors available. We explore the properties of these acceptors, from the point of view of achieving stable semi-insulating layers, which are essential in many device structures. Using hybrid density functional theory, we obtain the comprehensive first-principles results for a variety of deep-acceptor impurities in Ga_2O_3. Among the impurities examined, nitrogen on an oxygen site and magnesium on a gallium site have particularly low formation energies, making them prime candidates for acceptor doping. Closer inspection of various configurations shows that Mg can incorporate not only on Ga sites (where it acts as a deep acceptor under n-type conditions) but also on O sites, where it acts as a deep donor. Mg interstitials adopt a split-interstitial configuration, sharing a site with a host Ga atom. Similarly, N substituting on an O site acts as a compensating center, but N can also incorporate on the Ga site. We evaluate the diffusivities of these species in the crystal by calculating migration barriers and considering which native defects assist in diffusion. We find that diffusion of N is dominantly assisted by O vacancies, while Mg diffusion is assisted by gallium interstitials. Diffusion of Mg proceeds with significantly lower activation energies than diffusion of N. Our results can be used to assess activation energies and diffusion mechanisms for other impurities in Ga_2O_3.

Its wide bandgap makes Ga_2O_3 an attractive material for a wide range of applications[1,2] ranging from UV photodetectors[3,4] to high-power electronics.[5–7] Control over carrier concentrations is essential for all these applications. A number of donor impurities are available for n-type doping, as shown both computationally[8–12] and experimentally.[13–15] However, there are no known methods that can lead to p-type conductivity. Even if shallow acceptors were available, holes in Ga_2O_3 localize in the form of small polarons.[16] In addition, the investigations of acceptors that have been carried out to date identified only deep acceptors.[5,17–21]

However, deep acceptors are still useful. Not-intentionally doped Ga_2O_3 usually displays unintentional n-type conductivity, and achieving high-resistivity or semi-insulating layers requires adding acceptor impurities that will pin the Fermi level far from the band edges. Wong *et al.* demonstrated this could be achieved by ion implantation of Mg or N.[20] The purpose of introducing these impurities is to make them active as deep acceptors, which requires substitution on the Ga site for Mg or substitution on the O site for N. However, since the ion beams carry substantial energy, it is possible that higher-energy configurations are formed. Post-implantation annealing is required to drive the impurities to the intended site and to anneal out implantation damage; during this process, the impurities will diffuse.

Control of the doping process thus requires a solid understanding of the various configurations in which the impurities can be incorporated in the lattice, the relevant migration barriers, as well as the mechanisms by which

diffusion occurs. Accurate information about impurity diffusion is very important for device fabrication. Sufficiently high diffusivity is needed for acceptors to be properly incorporated in the lattice either by a solid-state diffusion process or by a post-growth anneal after implantation. On the other hand, too large a diffusivity might lead to acceptors moving out of the intended semi-insulating layer. The work reported in this paper is aimed at generating the information about the energetics of various configurations of acceptor impurities (including substitutional and interstitial sites), about complexes, and about migration barriers and diffusion mechanisms.

We address these issues by performing first-principles investigations of various acceptor impurities in Ga_2O_3. A comprehensive evaluation of a large number of candidate impurities reveals that they all are amphoteric, with deep (0/−) transition levels [more than 1.3 eV above the valence-band maximum (VBM)], and that the ones that are most likely to incorporate and to electrically act as deep acceptors are Mg substituting on Ga sites (Mg_{Ga}) and N substituting on O sites (N_O). Based on these results, we performed in-depth studies of Mg and N, evaluating various substitutional and interstitial configurations in the lattice as well as the formation of complexes. We find that "wrong-site substitution" (Mg on O sites or N on Ga sites) leads to deep-donor states. Interstitials also behave as donors when the Fermi level is low in the gap. A detailed analysis shows that both Mg and N doping do lead to Fermi levels deep in the gap, indicating that these dopants give rise to semi-insulating material. Finally, diffusion mechanisms are identified and the barriers for impurity migration determined. We find that Mg has lower migration barriers than N.

We use density functional theory as implemented in the Vienna Ab initio Simulation Package (VASP),[22] using projector augmented wave potentials[23] with an energy cutoff of 400 eV and a $2 \times 2 \times 2$ **k**-point grid in a 120-atom $3 \times 2 \times 2$ supercell. To accurately model the electronic and structural properties of Ga_2O_3, we use the HSE06 hybrid functional,[24] with a mixing parameter of 35%, which has been shown to yield very good results for lattice parameters and band structure.[25] Formation energies are calculated using the method outlined in Ref. 26. Chemical potentials are referenced to Ga bulk metal and O_2 molecules, thus setting the Ga-rich (O-poor) and Ga-poor (O-rich) limits through the enthalpy of formation of Ga_2O_3 (calculated to be –10.73 eV). For the impurities, we choose conditions corresponding to the solubility limit. For nitrogen, this implies equilibrium with N_2 molecules (under O-rich conditions) or with GaN (under Ga-rich conditions). For acceptor candidates on the Ga site, we considered the limiting oxide phases, i.e., the binary oxides,[27] the spinel phases MGa_2O_4 for M = Be, Mg, Zn, and Cd, and the MGa_4O_7 phases for M = Sr and Ca. Note that these O-rich and Ga-rich conditions are unlikely to be realized experimentally, but they act as the extreme limits: in reality, the results will be between these limits. Migration barriers were calculated using the climbing image nudged-elastic band (NEB) method.[28] All structures were visualized using the VESTA package.[29]

The ground-state crystal structure of Ga_2O_3 is the monoclinic β-gallia phase. This structure contains two inequivalent Ga positions, a tetrahedrally coordinated Ga(*I*) and an octahedrally coordinated Ga(*II*) position, and three inequivalent O positions: O(*I*) is threefold coordinated to 2 Ga(*II*) and 1 Ga(*I*) atoms. O(*II*) is also threefold coordinated but to 2 Ga(*I*) and 1 Ga(*II*) atom. The third O position [O(*III*)] is fourfold coordinated.

A survey of candidate acceptor impurities in Ga_2O_3 was recently performed by one of the present authors,[18] showing that all acceptor levels are deep. Moreover, for Fermi levels close to the VBM, these impurities actually behave as donors. In typical unintentionally *n*-type-doped material, incorporation of these impurities will drive the Fermi level down toward the (0/−) transition level. In the present work, we report new information about formation energies. Figure 1(a) shows that N can substitute on the O sites with low formation energies for Ga-rich conditions. We also considered P substituting on the

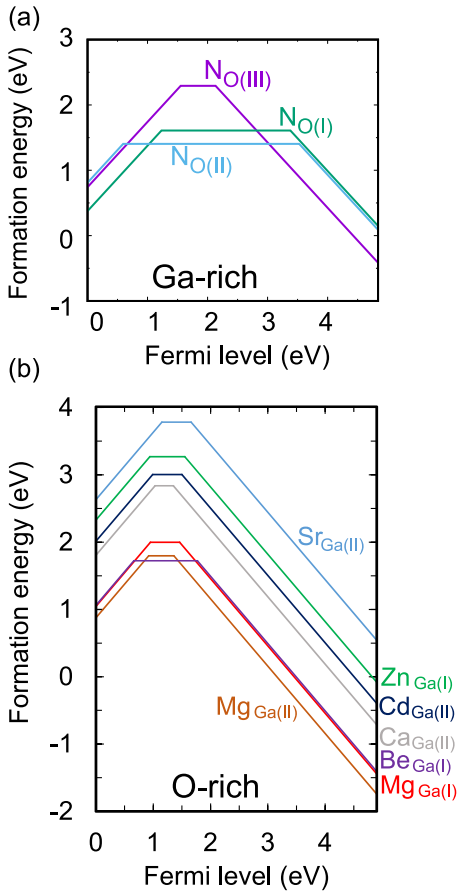

FIG. 1. Calculated formation energies as a function of the Fermi level for (a) N on the three inequivalent O sites and (b) Be, Mg, Ca, Sr, Zn, and Cd on the Ga site; for clarity, we only show the results for substitution on the Ga site with lowest energy, except for Mg where we show both. Fermi levels range from the VBM to the conduction-band minimum (CBM). Slopes indicate the charge state, and kinks in the curves correspond to charge-state transition levels.

oxygen site, but its formation energy is more than 2 eV higher than that of N_O.

Among impurities substituting on the Ga site in O-rich conditions [Fig. 1(b)], Mg has the lowest formation energy, for both types of Ga sites. Be is also low in energy when substituted on the Ga(I) site but is 1.17 eV higher in energy on the Ga(II) site. This difference is caused by the small ionic size of Be: on the tetrahedrally coordinated Ga(I) site both Be and Mg form four bonds; however, on the octahedral Ga(II) site, Be can form only three Be–O bonds, while Mg can form six bonds. Figure 1 demonstrates that all the candidate impurities are essentially amphoteric: they can behave as donors as well as acceptors and exhibit two charge-state transition levels in the gap: a (0/−) level characteristic of their acceptor nature and a (+/0) level closer to the VBM.

We now focus on the acceptors with the lowest formation energies, which are the ones that can be introduced in the highest concentrations: N on the O site and Mg on the Ga site. We will examine other configurations in which these impurities can be incorporated in the lattice and investigate diffusion mechanisms.

The detailed results for Mg are shown in Fig. 2. In addition to incorporating on a Ga site (Mg_{Ga}), we find that Mg can substitute on O sites (Mg_O) with relatively low formation energies, particularly when the Fermi level is low in the gap. Mg_O acts as a deep donor. Mg interstitials have even lower formation energies and also act as donors. We examined various configurations, and found that the lowest-energy structure corresponds to a split interstitial (Mg_i^{split}), in which Mg shares a lattice site with a Ga atom [see Fig. 3(b)]. Alternatively, Mg_i^{split} can be regarded as a complex between Mg_{Ga} and Ga_i.

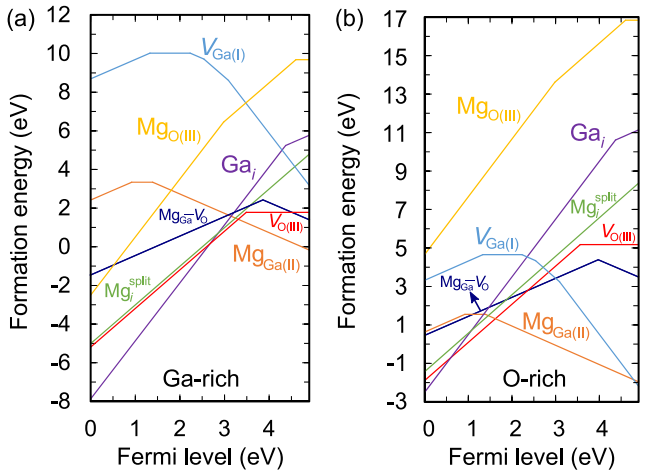

FIG. 2. Calculated formation energy under (a) Ga-rich conditions and (b) O-rich conditions of Mg in various configurations, as well as relevant point defects. The Mg configurations include Mg substituting on a Ga site (Mg_{Ga}), substituting on an O site (Mg_O), the Mg split interstitial (Mg_i^{split}), and a Mg_{Ga}–V_O complex. Point defects include interstitial Ga (Ga_i), Ga vacancies (V_{Ga}), and O vacancies (V_O).

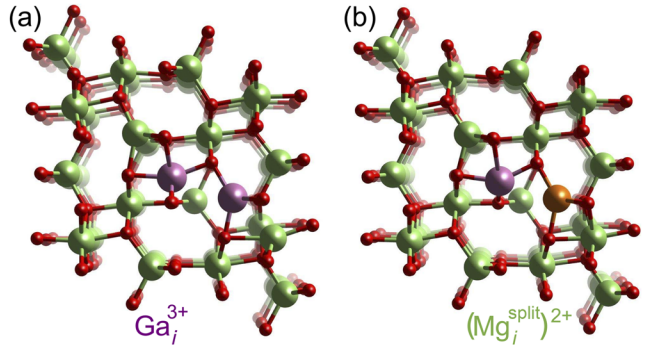

FIG. 3. Atomic configuration of (a) Ga_i^{3+} and (b) $\left(Mg_i^{split}\right)^{2+}$; both assume a split-interstitial configuration.

This configuration is 0.56 eV lower in energy than Mg_i occupying an interstitial position where it is surrounded by four O atoms. We will see below that the split-interstitial configuration plays an important role in diffusion.

Figure 2 also shows formation energies for native point defects that could be formed during an implantation process and that may play a role in diffusion. Ga vacancies are extremely unlikely to form when Mg is introduced with the intent of pinning the Fermi level far below the CBM: for the Fermi levels of interest, their formation energies are very high under both Ga-rich and Ga-poor conditions (Fig. 2). Ga interstitials (Ga_i) have low formation energies and act as deep donors. They form a split-interstitial configuration [see Fig. 3(a)]. Oxygen vacancies also have low energies when the Fermi level is far below the CBM although their energies would go up under less Ga-rich conditions [Fig. 2(b)].

With the knowledge of all these formation energies, we can deduce the effect of doping with Mg (in the absence of any other dopants). First, we consider Ga-rich conditions [Fig. 2(a)]. In that case, the defects with the lowest energy, along with Mg_{Ga}, are Ga_i, Mg_i^{split}, and V_O. Mg_{Ga} will act as an acceptor and be compensated by one of these other defects, which all act as donors; the resulting Fermi level will be located near the intersection of the lowest-energy donor and acceptor, roughly 1.5 eV below the CBM. Compensation could also occur with any (intentionally or unintentionally) incorporated shallow-donor impurity, in which case the Fermi-level position would also depend on the formation energy of the donor. The situation turns out to be very similar for O-rich conditions [Fig. 2(b)], with the same set of defects potentially compensating Mg_{Ga}. The main difference is that in this case, the Fermi level can be driven to lower positions in the bandgap than for Ga-rich conditions (as low as 3.3 eV below the CBM) although even here the Fermi level never approaches the Mg_{Ga} (0/−) acceptor level. Since Ga-rich and O-rich conditions represent extremes, we conclude that introducing Mg will indeed lead to a semi-insulating material.

The information contained in Fig. 2 also allows us to assess potential diffusion mechanisms for Mg. Gallium-vacancy assisted diffusion of Mg_{Ga} is unlikely given the Coulomb repulsion between the acceptor species and the high energy cost of the vacancies under the circumstances that are of interest here. Mg is much more likely to diffuse in a mechanism involving interstitials. Starting from Mg_{Ga} in a perfect lattice, this would not be feasible because creating a Mg_i from a Mg_{Ga} site requires the formation of a Ga vacancy, which costs too much energy. But Mg interstitials can relatively easily be formed. Mg_i^{split} associated with Ga(*I*) and Ga(*II*) sites have very similar energies, the octahedral site being higher by 0.1 eV. One can start from Mg_{Ga} in the presence of Ga interstitials (which have relatively low formation energies or could be formed during an implantation process). It is then energetically favorable for Mg_{Ga} and Ga_i to change places, resulting in formation of Mg_i^{split} [Fig. 3(b)]. The energy gain is 2.18 eV when starting from Mg in a tetrahedral site and 1.78 eV for an octahedral site. We note that during implantation, a certain fraction of Mg may also be directly generated in an interstitial configuration.

Using NEB, we calculated the barrier of moving the Mg atom in Mg_i^{split}. This barrier is small [0.56 eV for Mg_i^{split} associated with the Ga(*I*) site and 0.75 eV for the Ga(*II*) site], indicating fast migration as an interstitial. However, for the purposes of creating semi-insulating material, the Mg atom has to be incorporated on a Ga site. This will happen if it encounters a Ga vacancy, or by "dissociating" the split interstitial, forming first a Mg_{Ga}–Ga_i complex, from which the Ga interstitial can subsequently be dissociated. The barrier to go from Mg_i^{split} to Mg_{Ga}–Ga_i is higher than 2.3 eV. The resulting Ga_i also has low migration barriers (for example, 0.94 eV in the channel along the *b*-axis), so it will easily move through the material, potentially filling any Ga vacancies or diffusing out of the material.

We also assessed the potential impact of oxygen vacancies on Mg diffusion since they have low formation energies when the Fermi level is driven down (Fig. 2). Migration through oxygen vacancies would require the formation of Mg_O, which is at least 2.5 eV higher in energy compared to Mg_i^{split}; therefore, this pathway will not occur. We also calculated the formation energy of the Mg_{Ga}–V_O complex (included in Fig. 2). The complex has higher formation energy than the individual constituents. Our calculated binding energy is 0.91 eV. Mg_{Ga}–V_O complexes may form after cooldown but are unlikely to affect diffusion.

Next we consider how N incorporates in the Ga_2O_3 crystal structure. Figure 4 shows formation energies of relevant configuration and point defects. Oxygen vacancies have low formation energies when the Fermi level is well below the CBM, and therefore we also consider N_O–V_O complexes. The lowest-energy configuration of this complex has N on a fourfold oriented O(*III*) site, with an oxygen vacancy on a nearby O(*I*) site. This complex behaves as a deep donor. The oxygen interstitial (O_i), which is a deep acceptor,

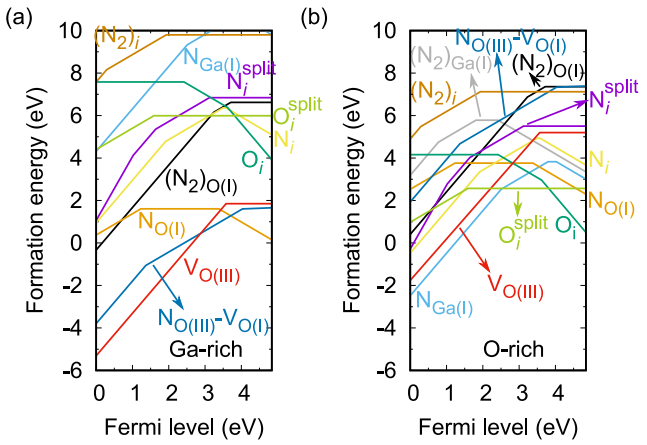

FIG. 4. Calculated formation energy under (a) Ga-rich conditions and (b) O-rich conditions for N substituting on an O(I) site [$N_{O(I)}$] or on a Ga(I) site [$N_{Ga(I)}$], the N interstitial (N_i), the N split-interstitial (N_i^{split}), an interstitial N_2 pair [$(N_2)_i$], and an N_2 pair substituting on an O(I) site [$(N_2)_{O(I)}$] or on a Ga(I) site [$(N_2)_{Ga(I)}$]. We also show an oxygen vacancy on the O(III) site [$V_{O(III)}$], an oxygen interstitial (O_i), an oxygen split-interstitial (O_i^{split}), and a $N_{O(III)}$–$V_{O(I)}$ complex. Only the lowest energy sites are shown.

has low formation energies in O-rich conditions. In these conditions, the oxygen split-interstitial (O_i^{split}), a deep donor, is also low in formation energy. N incorporating on the Ga site (N_{Ga}) occurs in positive charge states (acting as a donor) up to E_F = 3.80 eV and then becomes negatively charged (acting as an acceptor) when E_F is closer to the CBM. For Ga-rich conditions, its formation energy is high, but this lowers substantially in O-rich conditions, where it becomes the lowest energy defect.

We also considered N interstitials (N_i). They generally behave as deep donors (except when the Fermi level is high in the gap). They can also form a split-interstitial configuration (N_i^{split}), but this is always higher in energy. These interstitials can form complexes with substitutional nitrogen, forming nitrogen pairs. $(N_2)_{Ga}$ is always high in energy (even in the most favorable O-rich conditions), but $(N_2)_O$ is lower in energy and can be lower in energy than N_O when the Fermi level is in the lower portion of the bandgap. $(N_2)_O$ behaves as a deep donor.

The formation energies shown in Fig. 4 again allow us to predict an approximate position of the Fermi level in the case of doping with N (in the absence of any other dopants). For Ga-rich conditions, N_O will be compensated by V_O and/or the N_O–V_O complex, which are both deep donors. For O-rich conditions, N_O again acts as the acceptor, but under extreme O-rich conditions (which may be unrealistic), O_i will be even lower in energy, and the split-interstitial O_i^{split} is also low in energy. The latter occurs in a neutral charge state and will not influence the approximate Fermi level. N_{Ga} and V_O acts as donors. Therefore we see that under both Ga-rich and N-rich conditions, charge neutrality will compel E_F to be located

between 3.0 and 3.5 eV. In the presence of unintentional n-type dopants, the Fermi level could be somewhat higher. We keep these Fermi-level positions in mind when discussing nitrogen diffusion.

Diffusion of nitrogen can happen either via an interstitial or a vacancy mechanism. The vacancy mechanism is based on the formation of N_O–V_O complexes, which we found to form quite easily, particularly under Ga-rich conditions (Fig. 4). Within such a N_O–V_O complex, the barriers for N to jump into the neighboring vacancy are around 3.70 eV. The barriers for migration of O vacancies by itself were recently found to be between 1.2 and 4.0 eV, depending on charge state and specific migration pathway.[30] It is therefore not surprising that the combined barrier of moving N and O vacancies is similar in magnitude.

Interstitial migration can proceed with significantly lower barriers: in the N_i^- charge state, which is stable when E_F is above 3.57 eV, the interstitial has an extremely low migration barrier of 0.2 eV for migration along the b-axis. The other charge states also have low barriers. However, N_i has a high formation energy (higher than 5 eV for E_F above 3 eV), which will cause the overall diffusion activation energy to be very high. In fact, in the presence of oxygen vacancies (and for E_F above 3 eV), nitrogen interstitials can lower their energy by more than 5 eV by incorporating on an O site (Fig. 4). Diffusion of nitrogen via an interstitial mechanism is thus unlikely, and the vacancy mechanism will be preferred.

We now discuss our results in light of recent experimental measurements,[20] where it was found that after ion implantation, N does not diffuse at 1100 °C and starts diffusing only at 1200 °C, while Mg starts diffusing already at 800 °C. To connect these temperatures to calculated activation energies, we invoke transition state theory:[31] the rate of dopant hopping Γ is given by $\Gamma = \Gamma_0 \exp(-\frac{E_A}{k_B T})$, where E_A is the diffusion activation energy (which is the sum of the migration barrier and the formation energy of the defect assisting in the diffusion), k_B the Boltzmann factor, and T the temperature. We use 10^{13} as a typical prefactor. For N, we then obtain that the observed barrier is 3.87 eV, which agrees well with N migration through a vacancy-assisted process. For Mg, the observed barrier is 2.84 eV. This agrees well with the activation energy for an interstitial process, for which our calculated migration barrier is 0.56 or 0.75 eV, to which the formation energy of a Ga interstitial should be added. For the expected Fermi levels (see above), this formation energy is slightly above 2 eV.

In conclusion, we have performed a detailed study of candidate acceptors in β–Ga_2O_3. All considered dopants lead to deep acceptor levels, more than 1.3 eV above the VBM. This highlights the extreme challenges in ever realizing p-type dopable Ga_2O_3.[16–18] However, these dopants still provide utility in achieving highly insulating layers in electronic devices. Since N on O sites and Mg on Ga sites were found to have the lowest formation energies, we focused on these dopants. N on Ga sites or Mg on O sites can also form and act as donors, and both N and Mg interstitials are donors with low formation energies. Mg interstitials resemble the structure of the native split interstitial. Both Mg and N dopants lead to Fermi levels deep in the gap (at least 1 eV below the CBM). The information about Fermi-level positions, which cannot be obtained experimentally for semi-insulating material, is valuable for device design.[32] We also studied diffusion, finding that Mg diffusion is assisted by interstitials and N diffusion by vacancies. Our predicted diffusion activation energy is significantly lower in the case of Mg, and these activation energies agree quantitatively with the temperatures at which diffusion has been experimentally observed.[20] More generally, the results for formation energies and migration energies reported here can be used to assess mechanisms and activation energies for diffusion of other impurities in Ga_2O_3. The results can be easily extended to diffusion of other acceptor dopants, such as Be_{Ga}, but can also be applied to donor-type dopants, such as Si_{Ga}, which would likely diffuse by a V_{Ga}-assisted mechanism.

H.P. was supported by the Air Force Office of Scientific Research (No. FA9550-18-1-0059) and by the GAME MURI (No. FA9550-18-1-0479). J.L.L. was supported by the Office of Naval Research (ONR) Basic Research Program. This work was partially performed under the auspices of the U.S. DOE by Lawrence Livermore National Laboratory under Contract No. DE-AC52-07NA27344 and supported by the Critical Materials Institute, an Energy Innovation Hub funded by the U.S. DOE, Office of Energy Efficiency and Renewable Energy, Advanced Manufacturing Office. Computing resources were provided by the Center for Scientific Computing at the CNSI and MRL: an NSF MRSEC (No. DMR-1121053) and No. NSF CNS-0960316, by the Extreme Science and Engineering Discovery Environment (XSEDE), which is supported by NSF Grant No. ACI-1053575, and by the DoD Major Shared Resource Center at AFRL.

REFERENCES

[1] J. Y. Tsao, S. Chowdhury, M. A. Hollis, D. Jena, N. M. Johnson, K. A. Jones, R. J. Kaplar, S. Rajan, C. G. Van de Walle, E. Bellotti, C. L. Chua, R. Collazo, M. E. Coltrin, J. A. Cooper, K. R. Evans, S. Graham, T. A. Grotjohn, E. R. Heller, M. Higashiwaki, M. S. Islam, P. W. Juodawlkis, M. A. Khan, A. D. Koehler, J. H. Leach, U. K. Mishra, R. J. Nemanich, R. C. N. Pilawa-Podgurski, J. B. Shealy, Z. Sitar, M. J. Tadjer, A. F. Witulski, M. Wraback, and J. A. Simmons, Adv. Electron. Mater. **4**, 1600501 (2018).

[2] S. J. Pearton, J. Yang, P. H. Cary, F. Ren, J. Kim, M. J. Tadjer, and M. A. Mastro, Appl. Phys. Rev. **5**, 011301 (2018).

[3] A. K. Chandiran, N. Tetreault, R. Humphry-Baker, F. Kessler, E. Baranoff, C. Yi, M. K. Nazeeruddin, and M. Grätzel, Nano Lett. **12**, 3941 (2012).

[4] T. Minami, Y. Nishi, and T. Miyata, Appl. Phys. Express **6**, 044101 (2013).

[5] M. Higashiwaki, K. Sasaki, A. Kuramata, T. Masui, and S. Yamakoshi, Appl. Phys. Lett. **100**, 013504 (2012).

[6] K. Sasaki, M. Higashiwaki, A. Kuramata, T. Masui, and S. Yamakoshi, IEEE Electron Device Lett. **34**, 493 (2013).

[7] W. S. Hwang, A. Verma, H. Peelaers, V. Protasenko, S. Rouvimov, H. (Grace) Xing, A. Seabaugh, W. Haensch, C. Van de Walle, Z. Galazka, M. Albrecht, R. Fornari, and D. Jena, Appl. Phys. Lett. **104**, 203111 (2014).

[8]J. B. Varley, J. R. Weber, A. Janotti, and C. G. Van de Walle, Appl. Phys. Lett. **97**, 142106 (2010).
[9]J. L. Lyons, D. Steiauf, A. Janotti, and C. G. Van de Walle, Phys. Rev. Appl. **2**, 064005 (2014).
[10]H. Peelaers and C. G. Van de Walle, Phys. Rev. B **94**, 195203 (2016).
[11]P. Deák, Q. Duy Ho, F. Seemann, B. Aradi, M. Lorke, and T. Frauenheim, Phys. Rev. B **95**, 075208 (2017).
[12]T. Zacherle, P. C. Schmidt, and M. Martin, Phys. Rev. B **87**, 235206 (2013).
[13]E. Ahmadi, O. S. Koksaldi, S. W. Kaun, Y. Oshima, D. B. Short, U. K. Mishra, and J. S. Speck, Appl. Phys. Express **10**, 041102 (2017).
[14]D. Gogova, M. Schmidbauer, and A. Kwasniewski, CrystEngComm **17**, 6744 (2015).
[15]D. Gogova, G. Wagner, M. Baldini, M. Schmidbauer, K. Irmscher, R. Schewski, Z. Galazka, M. Albrecht, and R. Fornari, J. Cryst. Growth **401**, 665 (2014).
[16]J. B. Varley, A. Janotti, C. Franchini, and C. G. Van de Walle, Phys. Rev. B **85**, 081109(R) (2012).
[17]A. Kyrtsos, M. Matsubara, and E. Bellotti, Appl. Phys. Lett. **112**, 032108 (2018).
[18]J. L. Lyons, Semicond. Sci. Technol. **33**, 05LT02 (2018).
[19]J. R. Ritter, J. Huso, P. T. Dickens, J. B. Varley, K. G. Lynn, and M. D. McCluskey, Appl. Phys. Lett. **113**, 052101 (2018).
[20]M. H. Wong, C.-H. Lin, A. Kuramata, S. Yamakoshi, H. Murakami, Y. Kumagai, and M. Higashiwaki, Appl. Phys. Lett. **113**, 102103 (2018).
[21]Z. Galazka, K. Irmscher, R. Uecker, R. Bertram, M. Pietsch, A. Kwasniewski, M. Naumann, T. Schulz, R. Schewski, D. Klimm, and M. Bickermann, J. Cryst. Growth **404**, 184 (2014).
[22]G. Kresse and J. Furthmüller, Phys. Rev. B **54**, 11169 (1996).
[23]P. E. Blöchl, Phys. Rev. B **50**, 17953 (1994).
[24]J. Heyd, G. E. Scuseria, and M. Ernzerhof, J. Chem. Phys. **118**, 8207 (2003); **124**, 219906 (2006).
[25]H. Peelaers and C. G. Van de Walle, Phys. Status Solidi B **252**, 828 (2015).
[26]C. Freysoldt, B. Grabowski, T. Hickel, J. Neugebauer, G. Kresse, A. Janotti, and C. G. Van de Walle, Rev. Mod. Phys. **86**, 253 (2014).
[27]A. Jain, S. P. Ong, G. Hautier, W. Chen, W. D. Richards, S. Dacek, S. Cholia, D. Gunter, D. Skinner, G. Ceder, and K. A. Persson, APL Mater. **1**, 011002 (2013).
[28]G. Henkelman, B. P. Uberuaga, and H. Jónsson, J. Chem. Phys. **113**, 9901 (2000).
[29]K. Momma and F. Izumi, J. Appl. Crystallogr. **44**, 1272 (2011).
[30]A. Kyrtsos, M. Matsubara, and E. Bellotti, Phys. Rev. B **95**, 245202 (2017).
[31]G. H. Vineyard, J. Phys. Chem. Solids **3**, 121 (1957).
[32]I. Chatterjee, M. J. Uren, S. Karboyan, A. Pooth, P. Moens, A. Banerjee, and M. Kuball, IEEE Trans. Electron Devices **64**, 977 (2017).